Inhibiting effect of oxidized zirconium on parasitic cathodic reactions in the sodium chlorate process[†]
Part I: Hypochlorite reduction

F. HERLITZ*
Department of Chemical Engineering and Technology/Applied Electrochemistry, Royal Institute of Technology, SE-100 44 Stockholm, Sweden
(*author for correspondence at Eka Chemicals AB, PO Box 13000, SE-850 13 Sundsvall, Sweden)

Abstract

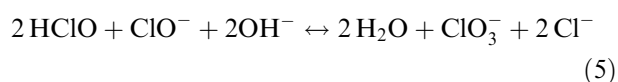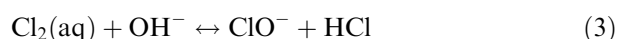To clarify the effect of oxidized zirconium on parasitic cathodic reactions in the chlorate process, electrochemical studies were carried out at laboratory scale. The techniques used were cyclic voltammetry and recording of polarization curves. In this paper the reduction of hypochlorite ions to chloride ions was studied. It is shown that oxidized zirconium cathodes reduces the rate of hypochlorite reduction, although not entirely inhibiting it, which is mainly related to a lowered active area due to the porous layer of zirconium dioxide. Further, it has also been shown that the oxidized samples are partly passivated, giving high overvoltages for the hydrogen evolution reaction. These overvoltages gradually decrease during cathodic polarization due to the simultaneous reduction of the zirconium oxide. Studies of the selectivity indicate that hypochlorite reduction occurs on the oxidised zirconium cathodes to a high extent, the thermal oxide being somewhat better. This further proves that zirconium oxide is not a suitable cathode material for the sodium chlorate process.

1. Introduction

One of the most important performance indicators in industrial electrolysis is the current efficiency. A high current efficiency is required to achieve a good economy for the process. The limiting factors are in most cases the potential range in which the electrodes work, and the composition of the electrolyte. One example is the chlorate process where sodium chlorate is produced according to the overall formula:

$$NaCl + 3\,H_2O \rightarrow NaClO_3 + 3\,H_2(g) \tag{1}$$
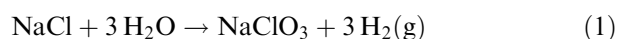
The reaction sequence can be described with the following reaction scheme:

$$2\,Cl^- \rightarrow Cl_2(aq) + 2\,e^- \tag{2}$$

$$Cl_2(aq) + OH^- \leftrightarrow ClO^- + HCl \tag{3}$$

$$ClO^- + H^+ \leftrightarrow HClO \tag{4}$$

$$2\,HClO + ClO^- + 2\,OH^- \leftrightarrow 2\,H_2O + ClO_3^- + 2\,Cl^- \tag{5}$$

where Reaction 2 takes place on the anode, while Reactions 3–5 are homogenous reactions occurring in the electrolyte. The cathode reaction according to Reaction 1 is the hydrogen evolution reaction (HER).

Parasitic reactions take place on both electrodes. Examples of anodic reactions are oxidation of chlorate to perchlorate, oxygen evolution or electrolytic formation of chlorate on the anode. The cathodic parasitic reactions are mainly the reduction of hypochlorite and chlorate ions:

$$ClO^- + H_2O + e^- \rightarrow Cl^- + 2\,OH^- \tag{6}$$

$$ClO_3^- + 3\,H_2O + 6\,e^- \rightarrow Cl^- + 6\,OH^- \tag{7}$$
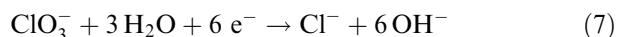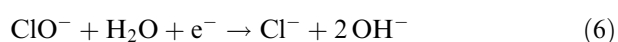
In the chlorate process, steel cathodes are now mainly used, and to suppress parasitic cathodic reactions sodium dichromate is added to the electrolyte. The addition of dichromate leads to the formation of a thin, selective film of chromium hydroxide on the cathode surface [1–5]. For environmental reasons a substitute needs to be found for dichromate addition and, at present, there are no clear alternatives. Instead it is of interest to use an electrode material with selective properties, allowing the HER but reducing the rate of other cathodic reactions. One possible material is zirconium(IV)oxide which has been shown to effectively

reduce the reduction rate of Ce(IV) to Ce(III) in sulphuric acid [6, 7] and the reduction of persulphate to sulphate [8]. It has been shown that a thermally grown oxide is more effective for inhibiting these two reductions than an electrochemically grown oxide [6–8]. In this work the effect of two types of oxidised zirconium, thermally and electrochemically oxidized, on the reduction of hypochlorite ions in sodium hydroxide solutions has been investigated by means of cyclic voltammetry, polarization curves and current efficiency measurements.

2. Experimental details

2.1. Electrodes

All zirconium samples were made from 1 mm thick sheets, quality ZR702 from Signer Titanium. The sheets were machined into quadratic pieces with a total area of 2 cm^2 for cyclic voltammetry and for polarization curve measurements and 8 cm^2 for current efficiency measurements. The pieces were then polished with abrasive paper, P240 from 3M, washed 30 min with detergent, Sodosil from Riedel-de-Haën, and then rinsed for 15 min with deionized water in an ultrasonic bath. One fraction of the zirconium electrodes was then thermally treated in air at 550 °C for 3 h, in a Solo furnace type 111–113, while another fraction was electrochemically oxidized. In the latter case the zirconium electrodes were fixed to a current collector, made of a stainless steel stick insulated with thermoretrecible plastic, and used as anode in a conventional 200 ml thermostatised glass cell at 25 °C. A platinum foil, area 10 cm^2, was used as cathode and separated from the anolyte with a fritted glass test tube. The electrolyte was 1 M H$_2$SO$_4$. The zirconium electrodes were then anodized potentiostatically at 70 V for 20 min. After the thermal treatment, which gives an oxide layer with a thickness of more than 1000 nm [8], a characteristic black colour appears on the electrodes surface and after the electrochemical treatment a characteristic golden colour appears on the electrode surface. In the latter case the thickness of the oxide is 200–300 nm.

The remaining part of the polished and washed zirconium electrodes were used without further treatment as reference samples. For some experiments a Pt foil, area 9.6 cm^2, was used as a working electrode.

The counter electrode was made of platinum and had a cylindrical configuration with wire mesh on its mantel area. As reference electrode a saturated calomel electrode (SCE), from Radiometer A/S in Copenhagen, was used and all potentials are measured and reported relative to the SCE.

2.2. Electrochemical cells

Two types of electrochemical cell were used: an undivided cell for cyclic voltammetry and polarization measurements and a divided cell for the current efficiency measurements. The undivided cell was a cylindrical 200 ml glass beaker with a jacket for circulating water from an external thermostat bath. In the lid, the working and counter electrodes were fixed, as well as a Luggin capillary for the reference electrode.

The divided cell was made of two 350 ml glass beakers separated by a Nafion® membrane and was placed in a thermostat bath. A Teflon lid was secured on top of the cathode compartment with an outlet for hydrogen gas.

2.3. Electrolytes and solutions

Sodium hydroxide solutions were prepared from Merck *pro analysi* crystals and water from a combined Milli-Q and Milli-RO15 water purification system from Millipore. Additions of NaOCl were made from a 1.0 M NaOCl + 0.1 M NaOH solution from BDH in the range 1–40 g dm^{-3}. All electrolytes, with and without additions of NaOCl, were 1.0 M with respect to OH$^-$. A stock solution of ferri–ferro cyanide was prepared and for some cyclic voltammetry experiments additions were made in equimolar ratio to 20 mM Fe(II)/Fe(III). All electrolytes were bubbled with nitrogen prior to the measurements and the electrolyte temperature was 25 °C in all experiments.

2.4. Electrochemical techniques

2.4.1. Cyclic voltammetry
All experiments were performed using a potentiostat PAR 273A, from EG&G PAR, controlled from a software package LabVIEW®, from National Instruments. Repetitive sweeps were made between a cathodic sweep limit, before the start of the hydrogen evolution reaction (HER), and an anodic sweep limit before the oxygen evolution reaction (OER) began. The sweeps usually had limits in the range from −1.6 V to 0.6 V and the sweep rate was 50 mV s^{-1}. All sweeps shown in the figures are pseudo-steady state sweeps, that is, the changes from a preceding sweep are negligible. Repetitive additions of NaOCl or Fe(II)/Fe(III) from the stock solutions were made when the sweeps with the earlier concentration had been recorded.

2.4.2 Polarization curves
Galvanostatic polarization curves were recorded using the instrumentation mentioned above. To compensate the potentials for the IR-drop a Nicolet 410 transient recorder was used. Potential transients were collected on the Nicolet 410 as an average of 20 transients differing in triggering time so the 50 Hz signal from the electric net was filtered out, as well as other noise. The transients were then analysed by fitting a relaxation equation to the part 5–100 μs after the current interrupt and extrapolating back to the triggering point [4]. The measurements were done step by step with 10 steps in each decade of current, beginning at 10 A m^{-2} and finishing at 3160 A m^{-2}, then returning to 10 A m^{-2}.

2.4.3. Current efficiency measurements

All current efficiency measurements were made by analysing the amount of hydrogen gas evolved from the cathode during a specific time period, usually one minute. The cathode was held at a constant current load, corresponding to a current density of -100 mA cm^{-2}, by means of a power source Oltronix B200. Repetitive additions of NaOCl from the stock solutions were made between each measuring point. All cathodes were pre-electrolysed for 4 h at -300 mA cm^{-2} in 1 M NaOH before the efficiency measurements were started.

3. Results and discussion

3.1. Cyclic voltammetry

3.1.1. Differences on voltammograms in NaOH

In Figure 1(a)–(c), characteristic cyclic voltammograms for nonoxidized, thermally oxidized and electrochemically oxidized zirconium are shown with and without additions of sodium hypochlorite. A large difference in the general shape of the voltammogram between the oxidized electrodes and the nonoxidised electrode can be seen. The start of the OER for nonoxidized zirconium can be seen in Figure 1(a) as well as the onset of the HER and there is no significant evidence for oxidation or reduction of an oxide layer on the zirconium. The

oxidation and reduction of the oxide are seen in Figure 1(b) and 1(c) for the two oxidised electrodes. An anodic peak is present in these figures at -0.3 V for both oxides. This peak probably corresponds to the point where the total amount of charge corresponds to the oxidation of earlier reduced zirconium dioxide sites and where the oxide film growth is limited due to decreased conductivity of the oxide layer. This effect can also be seen for electrodes that have been cathodically polarized for one hour or more.

3.1.2. Effect of hypochlorite

Addition of 1 g dm^{-3} NaOCl causes a small cathodic shift of the voltammogram at potentials more negative than -0.8 V. This shift is more or less parallel to the voltammogram with no NaOCl in the electrolyte, indicating that the mass transfer of the hypochlorite ion limits the reduction rate. An interesting comparison with a corresponding voltammogram for the hypochlorite reduction on platinum, Figure 1(d), can be made. For platinum, the hypochlorite reduction is known to have a low overvoltage [1]. A parallel shift of more than 1 V is obvious for potentials below 0.2 V in the platinum case and the hypochlorite reduction is definitely mass transfer controlled as there is a reduction peak before this parallel shift. There is no peak present for the nonoxidized zirconium which, together with the large difference in shift between the two metals, suggests
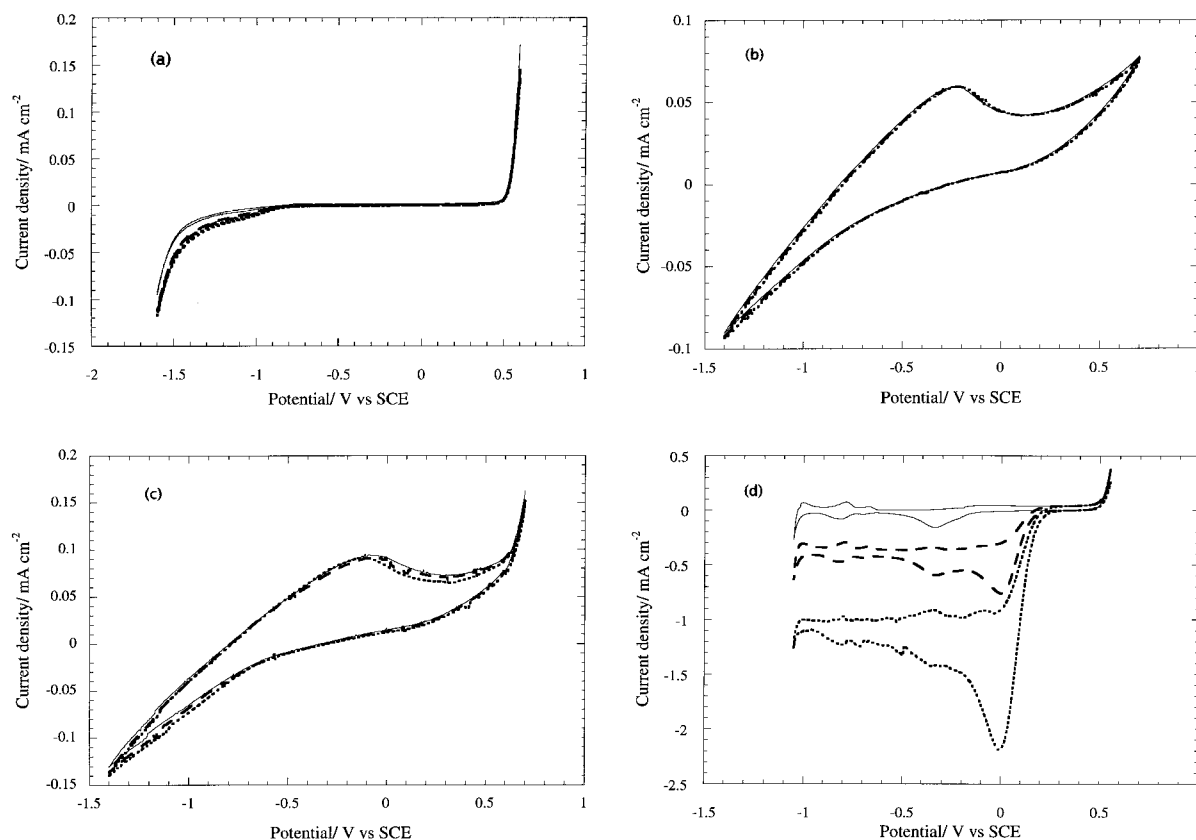

Fig. 1. Cyclic voltammograms recorded with a sweep rate of 50 mV s^{-1} at 25 °C in 1 M NaOH with additions of NaOCl. Sweep limits have been chosen as the on-set of hydrogen evolution and oxygen evolution for each electrode material. (a) Nonoxidized zirconium; (b) thermally oxidized zirconium; (c) electrochemically oxidized zirconium; (d) platinum. Key: (——), (– – –) 1 and ($\cdots\cdots$) 2 g dm^{-3} NaOCl.

that there is an effect which lowers the reduction rate on zirconium, but not entirely hinders the reduction. This can be explained by the existence of a thin oxide/hydroxide film [7] on the pure zirconium, which influences the reduction of hypochlorite. This is also supported by the fact that a further addition of NaOCl only gives a small shift of the voltammogram in Figure 1(a), while the shift for platinum, in Figure 1(d), is of the same magnitude as the previous one.

The effect of hypochlorite addition on oxidised samples can be seen in Figure 1(b) and (c). There is a very small shift, if any, indicating that the oxidized electrodes might have a similar effect, but stronger, as the zirconium electrode on the reduction of the hypochlorite ion. The broad oxidation and reduction peaks in the voltammograms together with the start of the HER make it difficult to estimate the exact magnitude of the hypochlorite reduction.

3.1.3. Ferri-/ferrocyanide
To verify the results from above, cyclic voltammetry experiments were carried out for the ferri-/ferrocyanide couple, which is a well-known reversible redox couple on platinum. In Figure 2(a), a reduction peak is found for platinum at 0.2 V and the reduction seem to continue at a limiting current density for more negative potentials, as was the case for the hypochlorite reduction on platinum in Figure 1(d). The shape of the curve

may be explained by the relatively high sweep rate, 50 mV s^{-1}, where mass transfer will be the rate-determining factor and not the electrode kinetics. For the pure zirconium sample in Figure 2(b) the reduction of ferricyanide ions starts at -0.6 V. In this case there is no peak but instead the cathodic current increases, almost reaching a level corresponding to the apparent limiting current density of platinum. It is not possible to see an oxidation peak for the ferrocyanide ion, explained by the higher overvoltage for this reaction on zirconium. The cyclic voltammograms for the oxidised zirconium samples, Figure 2(c) and (d), indicate a low reduction of ferricyanide. It is evident that the oxide film has an effect on the reduction of larger ions like hypochlorite and ferricyanide.

3.2. Polarisation curves

In Figure 3(a) and (b), polarization curves in 1 M NaOH for the nonoxidized zirconium and the thermal zirconium dioxide can be found. The behaviour of the electrochemical oxide is very similar to the thermal dioxide and the discussion below is valid for both types of oxides. Between each curve a cathodic polarisation at -100 mA cm^{-2} was applied. It is evident that the electrodes are becoming more active with respect to the HER with increasing polarization time. As the curves are recorded from low current densities to high
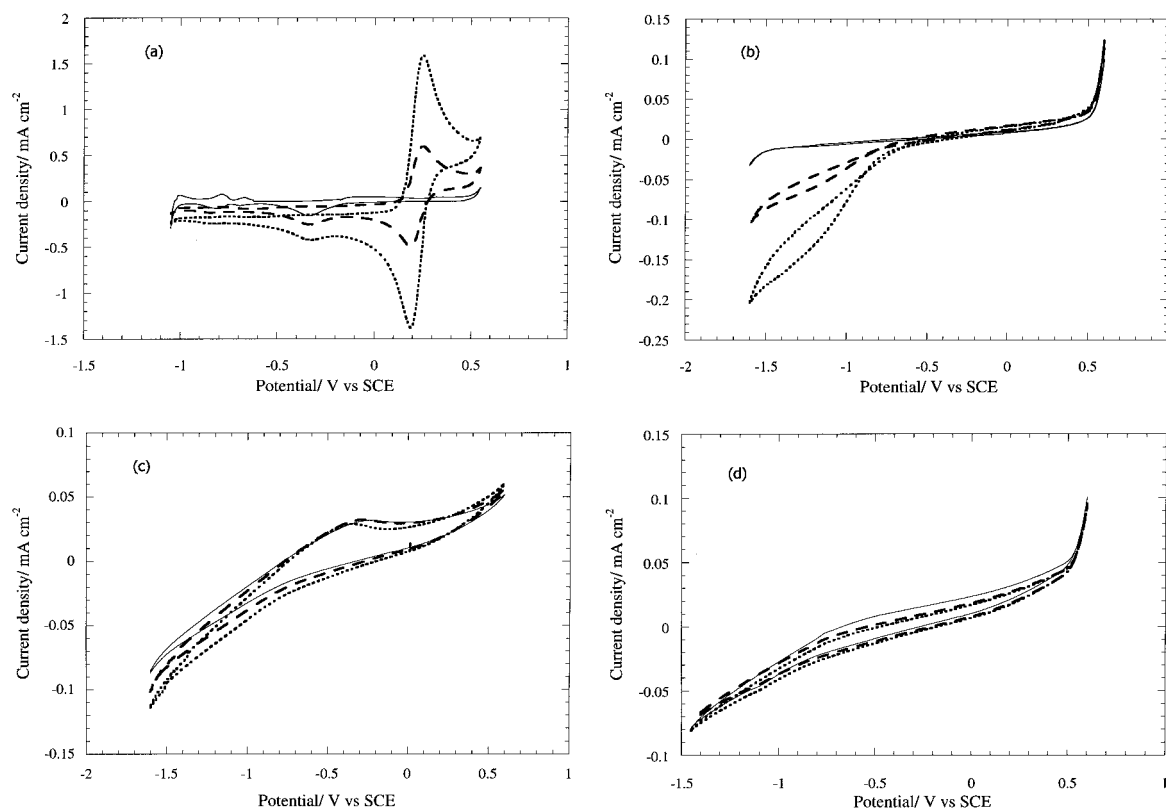

Fig. 2. Cyclic voltammograms recorded with a sweep rate of 50 mV s^{-1} at 25 °C in 1 M NaOH with additions of ferri-/ferrocyanide. Sweep limits have been chosen as the on-set of hydrogen evolution and oxygen evolution for each electrode material. (a) Platinum; (b) nonoxidized zirconium; (c) thermally oxidized zirconium; (d) electrochemically oxidized zirconium. Key: (——) 0, (– – –) 10 and (·····) 20 mM Fe(II)/Fe(III).
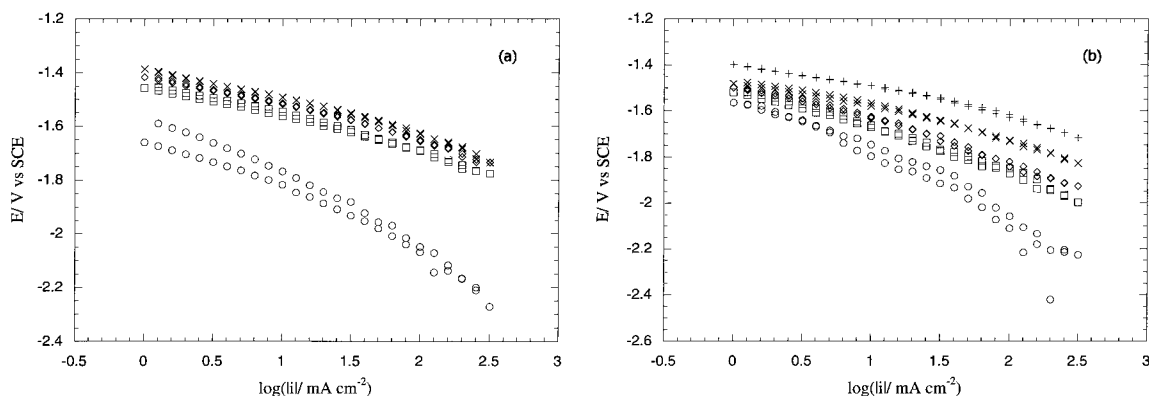
Fig. 3. IR-corrected polarization curves recorded at 25 °C in 1 M NaOH as a function of cathodic polarization time according to the legends, for example, 3 h_n indicates that the electrode been galvanostatically polarized for 3 h at a current density of −100 mA cm^{-2}. (a) Nonoxidized zirconium; Key: (○) 0, (□) 1, (◇) 2 and (×) 3 h_n. (b) Thermally oxidized zirconium; Key: (○) 0, (□) 1, (◇), (×) 3 and (+) 18 h_t.

current densities and back, a small hysteresis effect is seen for the first curve in each Figure. This indicates that there are a number of oxide sites that are more easily reduced. There is also a large decrease in overvoltage after only one hour of cathodic polarization, giving more proof of easily reduced oxide sites where the HER can proceed at lower overvoltages. Prolonged cathodic polarization gives a further reduction of the oxide, as can be seen in Figure 3(b) for the curve recorded after 18 h of cathodic polarization. The improvement from the initial curve is around 500 mV at the technical current density of −300 mA cm^{-2}. This can be explained as an increase in electrochemical active area due to increased porosity for the oxidized samples. It is interesting that the overvoltage is the same order of magnitude as for iron cathodes [4].

3.3. *Current efficiency measurements*

In order to compare the selectivity with respect to HER, current efficiency measurements were made in sodium hydroxide solution with additions of hypochlo-
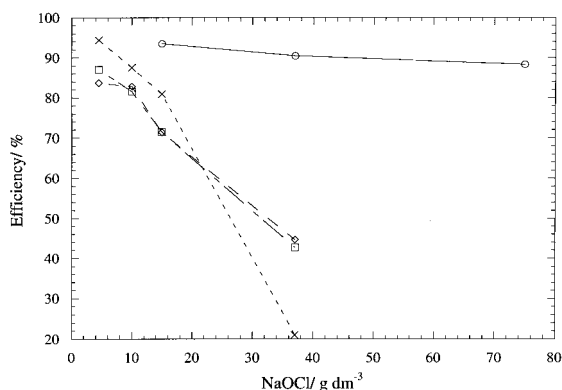
rite, see Figure 4. It is evident that hypochlorite reduction takes place on all materials. However, the thermal oxide has a significantly higher efficiency at high hypochlorite concentrations. This is also in accordance with the findings of Malherbe and Comninellis [6], Malherbe [7] and Vianin and Comninellis [8], who attributed this to the thicker oxide film formed in the thermal oxidation process. Lindbergh et al. [4] has shown that the presence of dichromate in the electrolyte, eliminates the hypochlorite reduction more or less completely. This is evidently not the case for oxidized zirconium.

4. Conclusions

This study has confirmed that zirconium oxide lowers the reduction rate of hypochlorite, but still a significant amount of hypochlorite is reduced. The thermal oxide has the highest selectivity for the HER, but as the oxide is reduced the selectivity decreases. As zirconium dioxide is a semiconductor, it has a passivating effect that initially gives high overvoltages. As the reduction of the oxide continues, the electrochemically active surface increases, the oxide becomes more porous and the overvoltage decreases significantly.

The major conclusion is that zirconium dioxide cannot be considered as an alternative to chromate additions into the chlorate electrolyte.

Acknowledgements

Fig. 4. The efficiency for hydrogen evolution in 1 M NaOH at 25 °C as a function of NaOCl concentration. Different electrode materials are indicated in the legend according to their chemical formula and by use of the abbreviations e and t for electrochemically oxidized zirconium and thermally oxidized zirconium, respectively. Key: (○) ZrO2t, (□) ZrO2e, (◇) Zr and (×) Pt.

References

1. G. Lindbergh and D. Simonsson, *J. Electrochem. Soc.* **137** (1990) 3094.

2. A. Ahlberg-Tidblad and G. Lindbergh, *Electrochim. Acta* **36** (1991) 1605.
3. G. Lindbergh and D. Simonsson, *Electrochim. Acta* **36** (1991) 1985.
4. G. Lindberg, D. Simonsson and A. Cornell, *Electrochim. Acta* **37** (1992) 1873.
5. A. Ahlberg-Tidblad and J. Mårtensson, *Electrochim. Acta* **42** (1997) 389.
6. Y. Malherbe and Ch. Comninellis, *J. Appl. Electrochem.* **24** (1994) 584.
7. Y. Malherbe, Thesis no. 1314, Swiss Federal Institute of Technology, Lausanne (1994).
8. L. Vianin and Ch. Comninellis, *Electrochim. Acta* **43** (1998) 1109–1112.